JMEPEG (1994) 3:501-513

Intermediate Shapes in Closed-Die Forging by the Backward Deformation Optimization Method (BDOM)

R. Srinivasan, G.H.K. Reddy, S.S. Kumar, and R.V. Grandhi

During closed-die forging, the billet is deformed through one or more intermediate shapes before achieving the final forged shape. Designers rely on handbooks and experience to choose a few of the limitless number of intermediate shapes that are possible. In this paper, a finite element method and optimization-based design technique for tracing the deformation back from the final to the initial shape is developed. Because plastic deformation is an irreversible process, no unique path exists between the initial and final shapes. Unlike previous backward tracing methods, the backward deformation optimization method (BDOM) selects the optimum path based on constraints placed on the deformation of the workpiece. Minimization of the variation in effective strain rate within the workpiece is used to determine the sequence of workpiece nodes to be detached from the die. Examples of intermediate shapes for the forging of a disk and a ball-joint socket demonstrate this design technique.

Keywords

backward deformation, closed die forging, finite element method, forging die design, shape optimization

1. Introduction

ENGINEERING components are frequently designed to meet specific functional requirements. These components may be shapes that are not directly forgeable, and their design is generally unalterable by the forging process design engineer. The engineer, therefore, has to design a forging process by considering a number of factors, including the shape of the finished part, the material, the forging equipment available (hammers, presses, etc.), the number of pieces being made, and the application (automotive, aerospace, etc.). The engineer first modifies the machined or finished part geometry taking into consideration the requirements of forging. This requires the addition of machining allowances, thermal expansion allowances if the part is to be warm or hot forged, draft angles, and fillet and corner radii to reduce stresses in the die. Next, the forging process is designed, selecting the temperature of forging (cold, warm, hot, or isothermal) based on the material, the forging speed, and the precision of the forging. Because the starting shapes of billets for forging operations are generally quite simple (circular, square, or rectangular bars) and the forging shape can be quite complex, the billet cannot be deformed to the final shape in a single forging step. In order to avoid problems, such as fold-overs, localized deformation (shear bands), improper die fill, and excessive die forces, the workpiece is deformed through one or more intermediate shapes before a product of the desired shape is formed. These intermediate shapes are referred to as the "buster," "blocker," or "finisher" shapes.

Conventional forging design relies heavily on forging handbooks and on the experience of the process designer. Handbooks provide guidelines to the engineer for making many of the decisions involved. Procedures for the design of the forging process have also been encoded into computer-based expert systems, such as Automatic Forging Design (AFD), Blocker Initial Design (BID), and DIE FORGE (Ref 1-4). These techniques have provided adequate designs, which have been validated through extensive physical modeling, i.e., a procedure entailing considerable expense and long lead times. Established forging processes that have been developed through conventional design methods are generally difficult to alter because of the costs involved in issues, such as modifying existing equipment, training of personnel, and certifying the new process. However, opportunities exist for applying systematic design methods to develop new processes for new materials and new products. This paper addresses the question of whether or not it is possible to optimize the intermediate shapes in a forging process based on the deformation characteristics of the deforming material.

R. Srinivasan, G.H.K. Reddy, S.S. Kumar, and **R.V. Grandhi,** Mechanical and Materials Engineering Department, Wright State University, Dayton, OH 45435, USA

2. Theory

The BDOM is a finite-element based technique. Several finite element programs for simulating metal deformation have been available since the early 1970s. The present analysis and methodology is based on the rigid viscoplastic method developed by Lee and Kobayashi (Ref 5), which was further extended to arbitrary shapes by Oh (Ref 6) in the program Analysis of Large Plastic Incremental Deformation (ALPID). The theoretical background for the rigid viscoplastic method is briefly discussed. Further details can be obtained from Lee and Kobayashi (Ref 5) and Kobayashi et al. (Ref 7).

The velocity field in a deforming rigid viscoplastic metal should satisfy the conditions of compatibility and incompressibility. At equilibrium, the functional Π, which is the difference between the rate of internal work of deformation and the external power, would have its minimum value. That is,

$$\Pi = \int_V \bar{\sigma}\,\dot{\bar{\varepsilon}}\; dV - \int_{S_f} F_i u_i dS \qquad \text{(Eq 1)}$$

At equilibrium,

$$\delta\Pi = \int_V \bar{\sigma}\,\delta\dot{\bar{\varepsilon}}\; dV + Q\int_V \dot{\varepsilon}_v \delta\dot{\varepsilon}_v dV - \int_{S_f} F_i \delta u_i dS = 0 \qquad \text{(Eq 2)}$$

The incompressibility requirement is incorporated into the above equation in the second term by introducing a large penalty constant, Q. S_f represents the surface area over which traction boundary conditions are present. For the forging problem, the surface traction is the frictional force between the workpiece and the die. At the die/workpiece interface, the velocity boundary condition is given in the direction normal to the interface by the die velocity, and the traction boundary condition along the interface is expressed as:

$$f_s = mkl \approx mk\frac{2}{\pi}\tan^{-1}\left(\frac{|u_s|}{u_0}\right)l \qquad \text{(Eq 3)}$$

where f_s is the frictional stress, l is the unit vector in the direction opposite to the sliding, u_s is the sliding velocity of a material node relative to the die, u_0 is a small positive number compared to u_s, and m is the friction factor for the constant shear force friction model (Ref 7).

In the matrix form, the governing equation for rigid viscoplasticity can be represented as:

$$[K]V = F \qquad \text{(Eq 4)}$$

where

$$[K] = \frac{\partial\Pi_D}{\partial v_i} + \frac{\partial\Pi_P}{\partial v_i} = \sum\left(\int_V \frac{\bar{\sigma}}{\dot{\bar{\varepsilon}}} P_{ij} dV + \int_V Q C_i C_j dV\right) \qquad \text{(Eq 5)}$$

and

$$F = \frac{\partial\Pi_{S_f}}{\partial v_i} = \sum\int_{S_f} mk\frac{2}{\pi} q_i \tan^{-1}\left(\frac{q_j u_{sj}}{u_0}\right) dS \qquad \text{(Eq 6)}$$

The velocity vector, V, the stiffness matrix, K, and the traction vector, F, are implicit functions of the die velocity. In addition, $[K]$ is nonlinear and material and process dependent. The solution to Eq 4 is, therefore, obtained iteratively. The velocity vector determined from the preceding set of nonlinear equations is used to update the geometry of the workpiece over a time step. During the "forward" simulation of metal deformation, nodes along the boundary will naturally come into contact with or separate from the die. The time step is, therefore, limited by such changes in the boundary conditions.

2.1 *Backward Deformation*

Hwang and Kobayashi (Ref 8, 9) developed a backward tracing method for determining the starting shape from which a given final shape could be forged. This method starts from the final product shape and a completely filled die, and the movement of the die is reversed in an attempt to reverse plastic deformation. During backward tracing, the workpiece boundary nodes are initially in contact with the die, and as the die is pulled back, nodes need to gradually separate from the die. The method iteratively checks if the new workpiece geometry, obtained after each nodal separation during backward simulation, results in the desired final shape, upon repeating the forward simulation. The starting shape or preform is obtained when all the boundary nodes have separated from the die. The procedure was demonstrated for the shell nosing problem in which the die shape was fairly simple, and the sequence in which nodes separate from the die is quite straightforward. This may not be true in the case of a general forging problem.

Plastic deformation is an irreversible process, and no natural or predefined path exists between a given billet (starting) shape and a product (finishing) shape. There are, therefore, a limitless number of paths between the finishing shape and the starting shape for backward deformation simulation. Specific paths may be selected by placing constraints on the backward deformation of the material. The BDOM combines the backward tracing method with numerical optimization techniques for determining a strategy to release nodes from an arbitrarily shaped die during reversed deformation. The overall objective is to minimize the variation in strain within a workpiece after forging. This objective is achieved by minimizing the strain rate variation during deformation.

2.2 *Strain-Rate Based Nodal Detachment*

Consider a workpiece that is being deformed by a moving die. The effect of die displacement is transmitted to the workpiece through the part of the bounding surface in contact with the die. The nodes in contact with the die have velocities U_1, U_2, U_3, etc. If the die displacement is reversed, and the nodes remain attached to the die, they would each move with a vertical velocity equal to that of the die (Fig. 1). However, the influence of the nodes on the distribution of velocities and strain rates in the workpiece may be quite different. The influence of each die contacting node can be determined by analytical design sensitivity calculations. A decision regarding which node is to be released from the die can then be made based on the resulting values of design parameters (Ref 10, 11).

The design variables for this problem are, therefore, U_i, the velocities of the die contacting workpiece nodes, which are all initially assumed to have the same value as the die velocity. The effective strain rates in the workpiece elements are used as design constraints. The design variables, U_i, that minimize the maximum deviation of the effective strain rates in the elements from the average strain rate are determined; i.e., find U_i to minimize H subject to the following inequality constraints:

$$\left|\dot{\bar{\varepsilon}}_k - \dot{\bar{\varepsilon}}_{avg}\right| \le H \quad k = 1, \ldots, n \qquad \text{(Eq 7)}$$

where $\dot{\bar{\varepsilon}}_k$ is strain rate in the kth element, $\dot{\bar{\varepsilon}}_{avg}$ is average strain rate, H is maximum difference between an element strain rate and the average strain rate, and n is number of elements.

Additional side constraints on the design variables, U_i, are:

$$0 \le U_i \le U_d \quad i = 1, \ldots, p \tag{Eq 8}$$

where U_d is the die velocity and p is the number of die contacting workpiece nodes. This problem, therefore, has p design variables and n design constraints, and can be reformulated as a sequential linear programming problem by linearizing effective strain rates:

$$\dot{\bar{\varepsilon}}_k = \dot{\bar{\varepsilon}}_{k0} + \sum_{i=1}^{p} \frac{\partial \dot{\bar{\varepsilon}}_k}{\partial U_i}\left(U_i - U_{i0}\right) \tag{Eq 9}$$

where $\dot{\bar{\varepsilon}}_{k0}$ is the effective strain rate in the kth element during the backward optimization process and U_{i0} is the velocity of the ith die contacting node before optimization. The initial design variables, U_{i0}, are the same as the die normal velocity.

The gradients of $\dot{\bar{\varepsilon}}_k$ with respect to U_i are calculated from the governing equation (Eq 4) and the relationships between nodal velocities and strain rates in an element, as follows (Ref 10, 11):

$$\frac{\partial V}{\partial U_i} = [K]^{-1}\left(\frac{\partial F}{\partial U_i} - \frac{\partial [K]}{\partial U_i} V\right) \tag{Eq 10}$$

The stiffness matrix and traction force vector derivatives are (Ref 7):

$$\frac{\partial [K]}{\partial U_i} V = \sum \int_V \left(\frac{1}{\dot{\bar{\varepsilon}}} \frac{\partial \bar{\sigma}}{\partial \dot{\bar{\varepsilon}}} - \frac{\bar{\sigma}}{\dot{\bar{\varepsilon}}^2}\right) \frac{1}{\dot{\bar{\varepsilon}}} P_{ik} V_k V_m P_{mj} \frac{\partial V_i}{\partial U_i} dV \tag{Eq 11}$$

and

$$\frac{\partial F}{\partial U_i} = \sum \int_s mk \frac{2}{\pi} q_i q_j \frac{u_0}{u_0^2 + (q_k u_{sk})^2} \frac{\partial}{\partial U_i} (V_j - U_j) dS \tag{Eq 12}$$

The effective strain rate is defined as:

$$\dot{\bar{\varepsilon}} = \sqrt{\frac{2}{3}\left(\dot{\varepsilon}_{ij} \dot{\varepsilon}_{ij}\right)} \tag{Eq 13a}$$

or

$$(\dot{\bar{\varepsilon}})^2 = \dot{\varepsilon}^T [D] \dot{\varepsilon} \tag{Eq 13b}$$

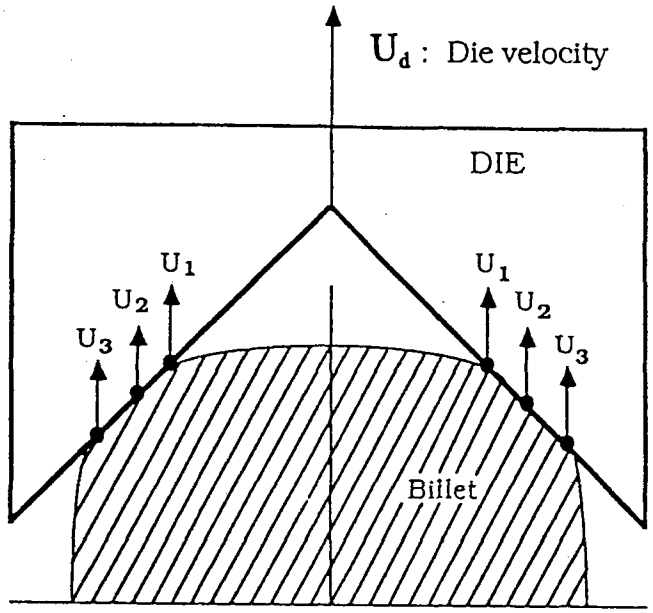

Fig. 1 Die velocity and design variables for BDOM

where $[D]$ is a diagonal matrix with components $\frac{2}{3}$ and $\frac{1}{3}$ corresponding to normal and engineering shear strain rates, respectively. The strain rate in each element is related to the nodal velocities through the strain rate matrix $[B]$; i.e.,

$$\dot{\varepsilon} = [B] v \tag{Eq 14}$$

Therefore,

$$(\dot{\bar{\varepsilon}})^2 = v^T [B]^T [D] [B] v = v^T [P] v \tag{Eq 15}$$

where $[P] = [B]^T [D] [B]$. Differentiating Eq 15 with respect to the design variable, U_i, gives:

$$\frac{\partial \dot{\bar{\varepsilon}}_k}{\partial U_i} = \frac{1}{\dot{\bar{\varepsilon}}_{k0}} v_k^T [P] \frac{\partial v_k}{\partial U_i} \tag{Eq 16}$$

where v_k is the nodal velocity vector for the kth element. The sensitivity of v_k to U_i is calculated from Eq 10. Equation 16 relates the change in the constraint function, i.e., the effective strain rate in an element, to the change in the design variable, i.e., the velocity of a node in contact with the die.

The optimization problem can be solved iteratively using simplex algorithm routines available in the IMSL package. This procedure ranks the die contact nodes based on their influence on the deformation of the workpiece by assigning them new velocities. The node with the smallest velocity has the least influence on the deformation and is detached. One node is detached from the die during each step, and the preceding geometry of the workpiece is then determined by backward tracing

from the current geometry. In order to ensure that this procedure does not deviate very far from linearity, the time step is limited by restricting the maximum change in effective strain in any element.

The process of backward deformation with optimization is repeated until all but one of the nodes have separated from the die. The geometry of the workpiece at this stage is considered to be one possible intermediate shape from which the final shape can be forged with the minimum variation in strain rate.

2.3 *Force-Based Nodal Detachment*

During a multiple-die forging operation, not all dies are moving simultaneously. However, during forward simulation, nodes do come into contact with such stationary dies. Therefore, an additional criterion needs to be established for nodal detachment during backward deformation. For this purpose, the force acting on the boundary nodes is determined. A node with no force is assumed to have detached from the die. The force-based nodal detachment criterion can be used in conjunction with the previously mentioned strain-rate based nodal detachment criterion.

2.4 *Grouping of Design Variables*

In principle, when the die is completely filled, the velocity of every node along the interface between the workpiece and the die is a design variable for the BDOM. Depending on the finite element mesh used to model the problem, the number of design variables can be quite large. Consequently, nodal detachment may occur at several separate locations along the die. This would result in an uneven workpiece boundary. In order to control the nodal detachment, the number of design variables is reduced by grouping several adjacent nodes along the boundary to form segments. The velocities of the nodes at the ends of the segments then become the design variables. One of these nodes is detached during each backward deformation step and is subsequently not considered as a design variable. As a result, the length of the segment to which this node belonged decreases. The number of design variables remains the same until a segment detaches completely from the die. The example of the single-die problem discussed in the following section illustrates the use of node grouping during optimization. Force-based nodal detachment is also carried out by grouping nodes in a similar manner.

3. Case Studies and Discussion

The applicability of the BDOM is demonstrated through several examples. Various problems are encountered when the forging is carried out in a single stage from the initial to the final shape. The examples show how the inclusion of an intermediate stage designed by BDOM avoids some of these problems and meets the constraints imposed by the optimization scheme.

3.1 *Forging of a Disk with an "H" Cross Section*

A typical disk geometry is shown in Fig. 2. The disk is axisymmetric and also is symmetric top to bottom. Parameters used to describe this shape are the web thickness, t, the rib height, H, and the rib width, B. The forging of this shape can be modeled either by considering just the top half and one die, or by considering both the top and bottom halves, and two dies.

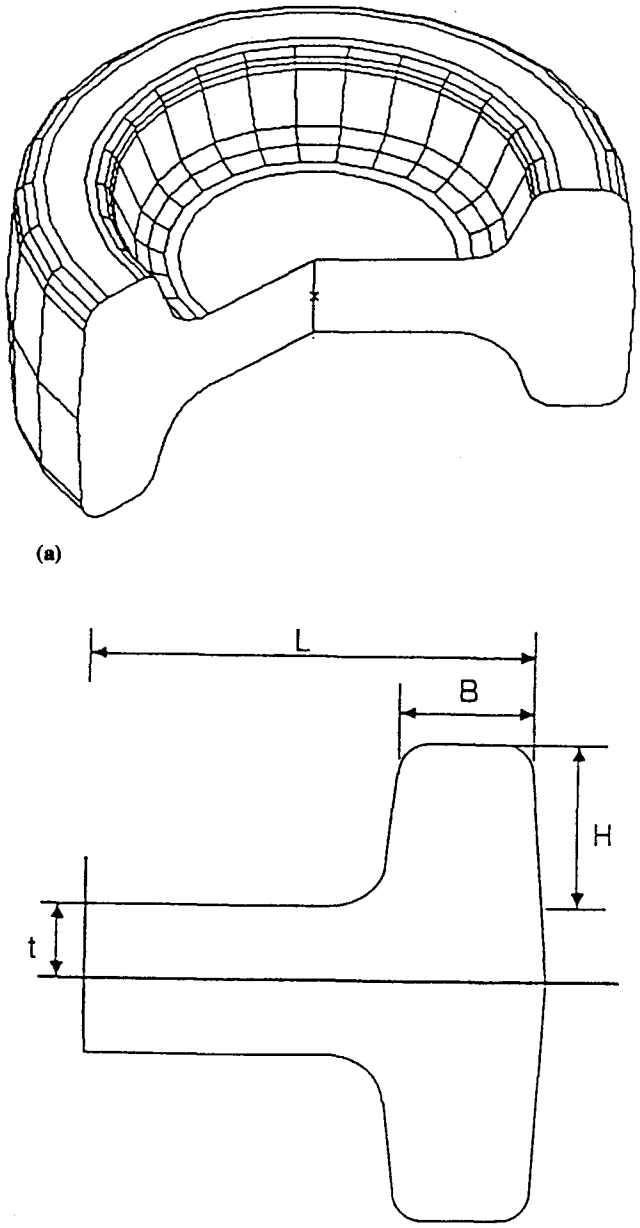

Fig. 2 Typical axisymmetric "H" cross section disk forging

The forging of a disk was simulated using the program ALPID. In the example shown in Fig. 3, symmetry about the horizontal plane was assumed. The domain was divided into mesh of 336 nodes and 297 elements, and a single moving (upper) die was used. When the forging is carried out in one stage,

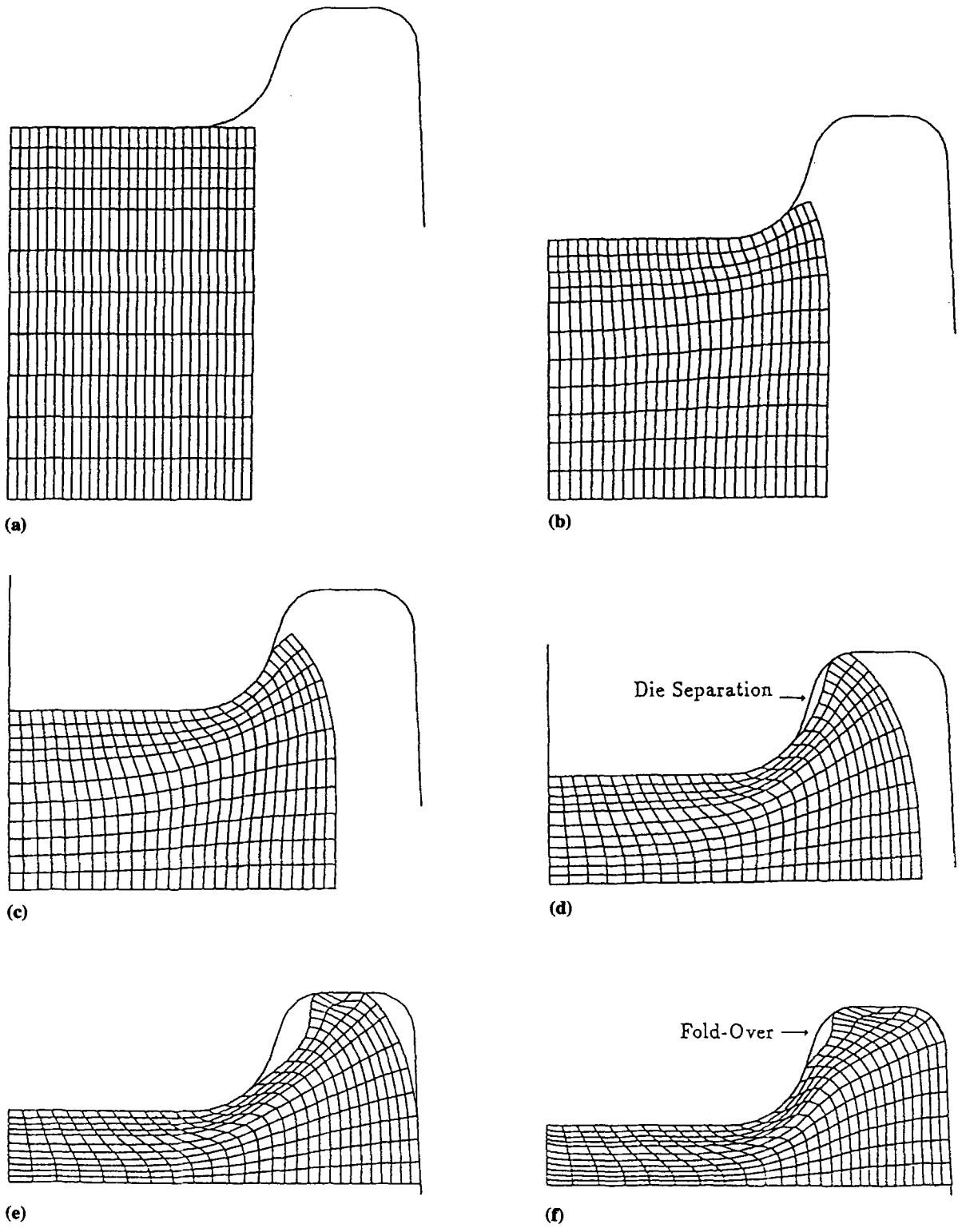

Fig. 3 Simulation of a single-stage forging of an "*H* " cross section disk

material can separate from the die (Fig. 3d) leading to the possibility of a fold over. This problem can be avoided by either redesigning the die, or by forging in more than one stage. The shape of the die for the intermediate stage for a two-stage forging operation is designed in the following two examples using BDOM.

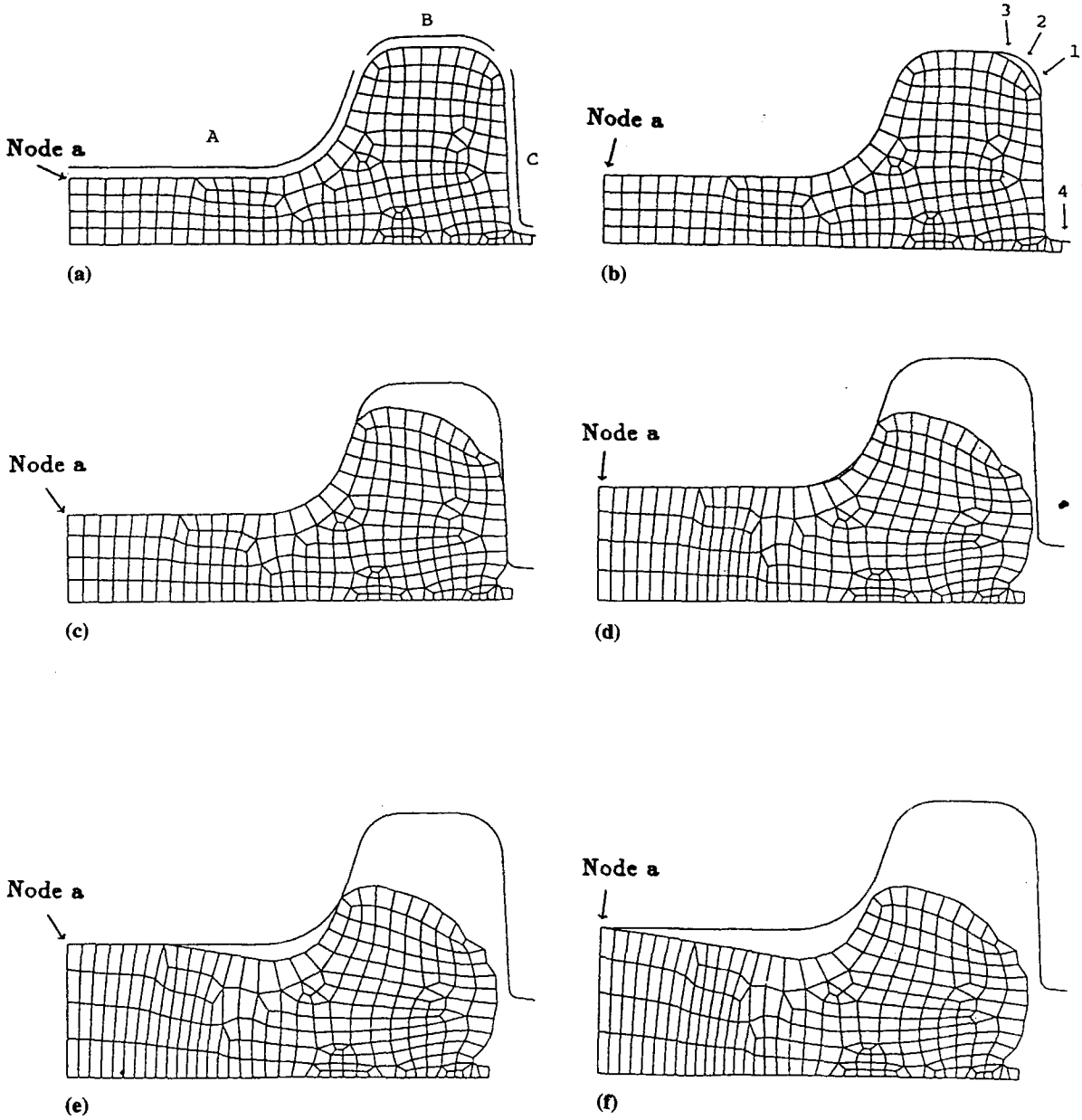

Fig. 4 Finite element grid shapes during backward deformation simulation using BDOM of the single die axisymmetric "*H* " cross section forging problem

Table 1 Strain rates variation before and after optimization for the one-die problem

Step	Maximum $\bar{\dot{\varepsilon}}_k$		Minimum $\bar{\dot{\varepsilon}}_k$		Average $\bar{\dot{\varepsilon}}_k$	
No.	Initial	Optimal	Initial	Optimal	Initial	Optimal
1	79.7712	29.2703	0.0523	0.1565	3.2270	1.9327
2	28.2244	17.6592	0.1578	0.1384	1.8820	1.5535
3	16.5594	11.7858	0.1370	0.0827	1.5322	1.3906
4	11.3894	11.1077	0.0869	0.1004	1.3735	1.3337
5	10.9692	7.67674	0.0986	0.1272	1.3169	1.2803

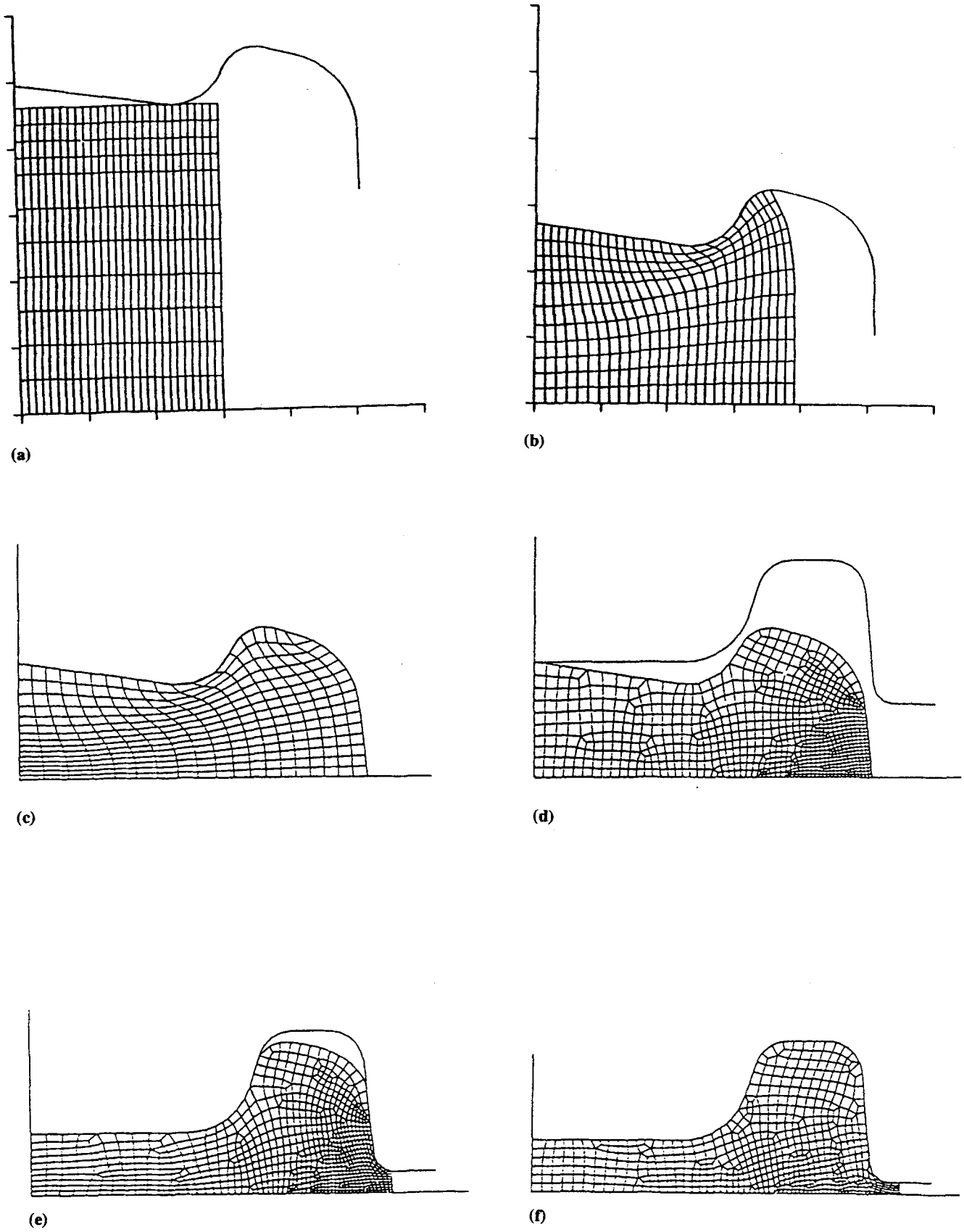

Fig. 5 Forward simulation of the single die "*H* " cross section forging in two stages using the optimized intermediate die shape

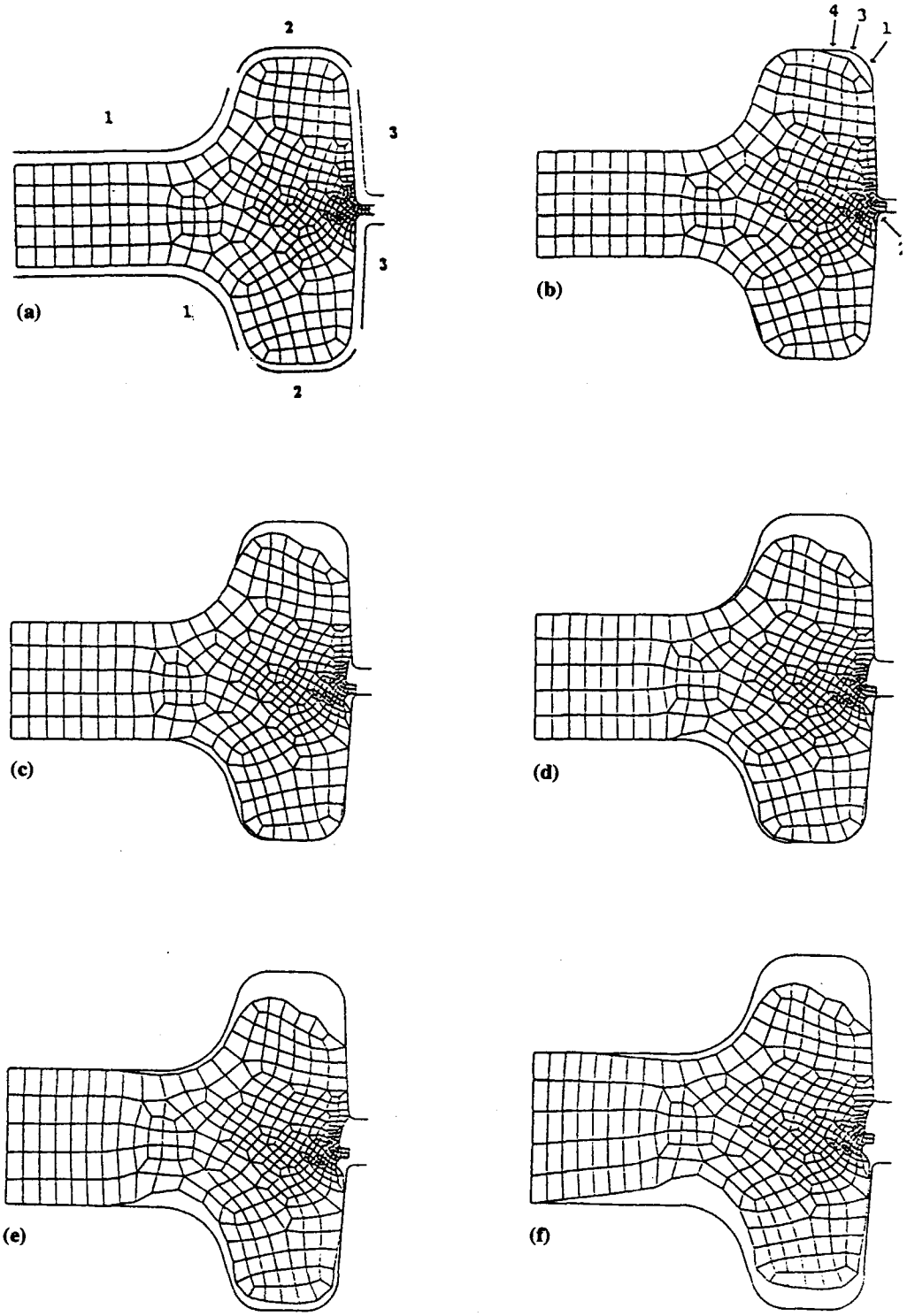

Fig. 6 Finite element grid shapes during backward deformation simulation using BDOM of the two die axisymmetric "*H* " cross section forging problem

3.1.1 Single-Die Problem

This case assumes symmetry about the horizontal plane, and only the top die is considered. To begin, the die is assumed to be completely filled, and a small amount of material is in the flash region. The finite element mesh is shown in Fig. 4a. The 42 nodes along the die contact boundary were grouped into segments A, B, and C with 21, 8, and 13 nodes, respectively. Node

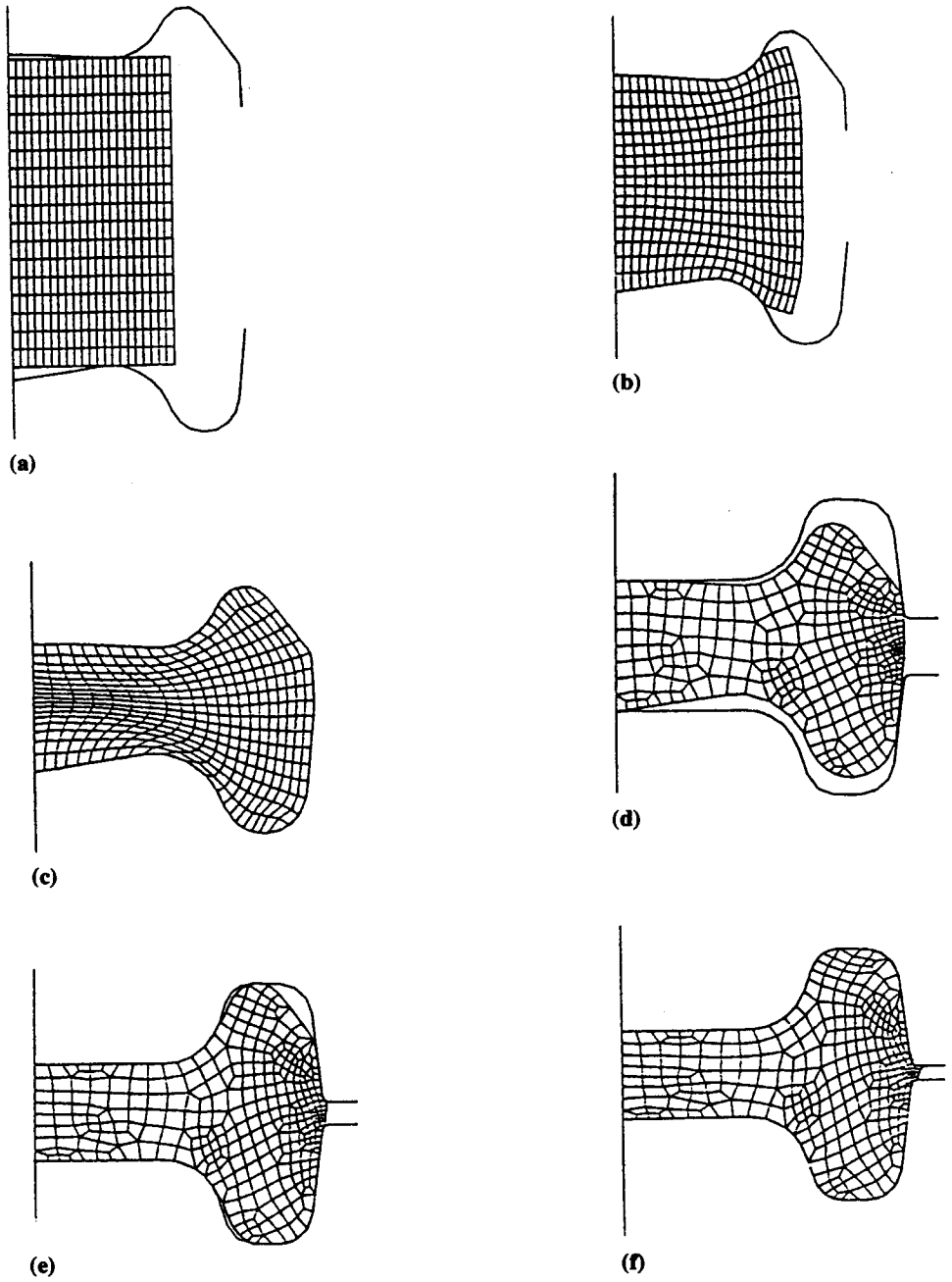

Fig. 7 Forward simulation of the two die "*H* " cross section forging in two stages using the optimized intermediate die shapes

Table 2 Strain rates variation before and after optimization for the two-die problem

Step	Maximum $\dot{\bar{\varepsilon}}_k$		Minimum $\dot{\bar{\varepsilon}}_k$		Average $\dot{\bar{\varepsilon}}_k$	
No.	Initial	Optimal	Initial	Optimal	Initial	Optimal
1	194.529	22.7577	0.1369	0.0949	11.183	1.9123
2	22.1986	22.0706	0.0896	0.0792	1.8628	1.5971
3	21.0064	16.9153	0.0761	0.0327	1.5861	1.4011
4	16.2173	16.1939	0.0324	0.0403	1.3988	1.3432
5	15.7145	14.8096	0.0503	0.0788	1.3396	1.3143

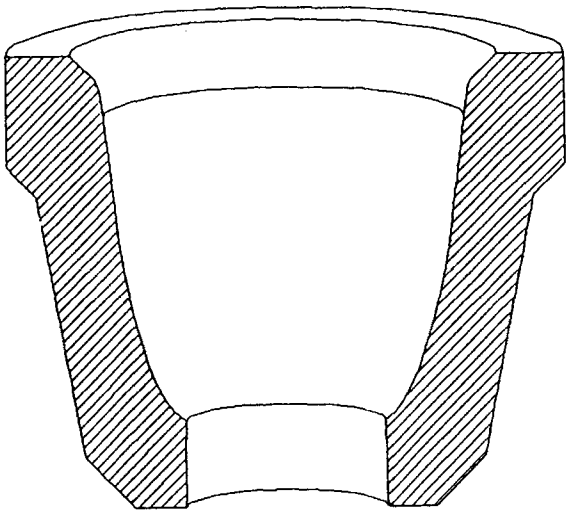

(a)

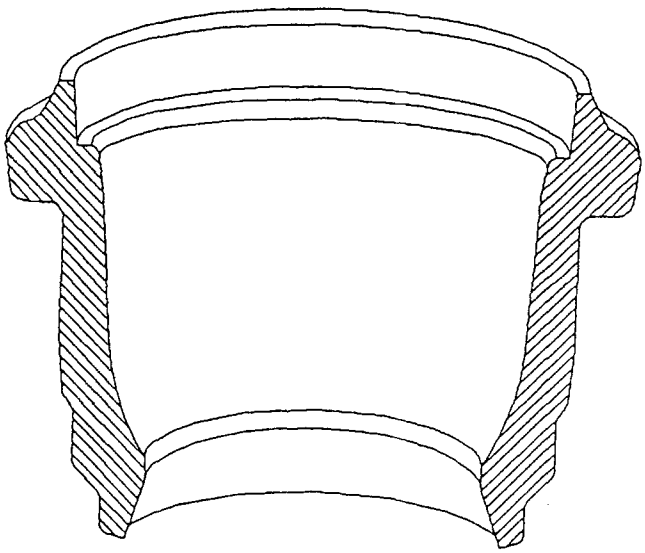

(b)

Fig. 8 Typical automotive ball-joint socket forging. (a) Preform shape. (b) Final forged shape

a at the end of segment A, which lies on the axis of symmetry, is assumed to stay in contact with the die, and its velocity is not a design variable. The remaining five nodes at the ends of the segments were the initial design variables.

At each step of the backward deformation simulation, the optimizer minimizes the range of strain rates in the elements by selecting the node to be detached from the die. After the first step, node 1 detaches from the die. Segment C now has 12 nodes, and the number of design variables remains 5, corresponding to the ends of the three segments. Figure 4b shows the geometry of the workpiece after the first four steps of backward deformation. Nodes 1, 2, 3, and 4 detach successively from the die. Table 1 shows the range of effective strain rates before and after each nodal detachment. In each case, the detachment of the node resulted in a decrease in the variation of strain rate.

Figure 4d shows the mesh geometry after all the nodes in segment C have separated from the die. At this step, the number of design variables is three, corresponding to the nodes at the ends of segments A and B, which have 16 and 2 nodes, respectively. The process of backward deformation was carried out until all but node **a** had separated from the die. The progress of backward deformation at selected steps is shown in Fig. 4(b)-(f). The workpiece geometry in Fig. 4f is the optimum intermediate shape in this case. Due to the small depression near the region of the flash, this shape is not directly forgeable. The boundary of the workpiece in Fig. 4f was smoothed, and depression was eliminated to create the intermediate die shape.

Figure 5 shows the deformation of a cylindrical billet to the designed intermediate shape in the first stage of forging (Fig. 5a-c), and then on to the final shape in the second stage. The finite element domain was remeshed between the first and second stages of forging. The domain was remeshed again after the step shown in Fig. 5e due to excessive mesh distortion in the flash region. Figure 5f shows that complete die fill has been obtained without a fold over.

The variation in total accumulated strain for the single-stage forging (Fig. 3) and the optimized two-stage forging (Fig. 5) was determined. The variance in strain was found to decrease by ~30% when two-stage forging was adopted. This implies that the deformation was more uniform when two-stage forging is used, thus satisfying the overall objective of BDOM.

3.1.2 Two-Die Problem

In this case the deformation is assumed to be not symmetric about the horizontal plane. Strain-rate based nodal detachment is applied on the top die, and force-based nodal detachment is applied on the bottom die. Figure 6a shows the grouping of nodes on the top and bottom dies. Successive workpiece shapes are shown in Fig. 6(b) to (f). Table 2 shows the variation in strain rate before and after the detachment of nodes 1, 2, 3, and 4. As for the one-die problem, the range of strain rates is reduced after optimization. Due to the nonlinear nature of the problem and the differences in the criteria used for nodal detachment from the upper and lower dies, there is no correspondence between the sequences of nodal separation from the two dies. The backward deformation stopped at the step shown in Fig. 6f when all nodes (except the axial node) had separated from the bottom die. This is the optimal intermediate geometry of the workpiece. This geometry is not symmetric about the horizontal plane and is not forgeable due to the depression in the region of the flash.

Figure 7a shows the intermediate die shapes obtained from Fig. 6f after smoothing and modifying the region near the flash. The shapes of the top and bottom dies at the intermediate stage of forging are different. Further, these shapes are different from the one obtained in the one-die problem discussed above.

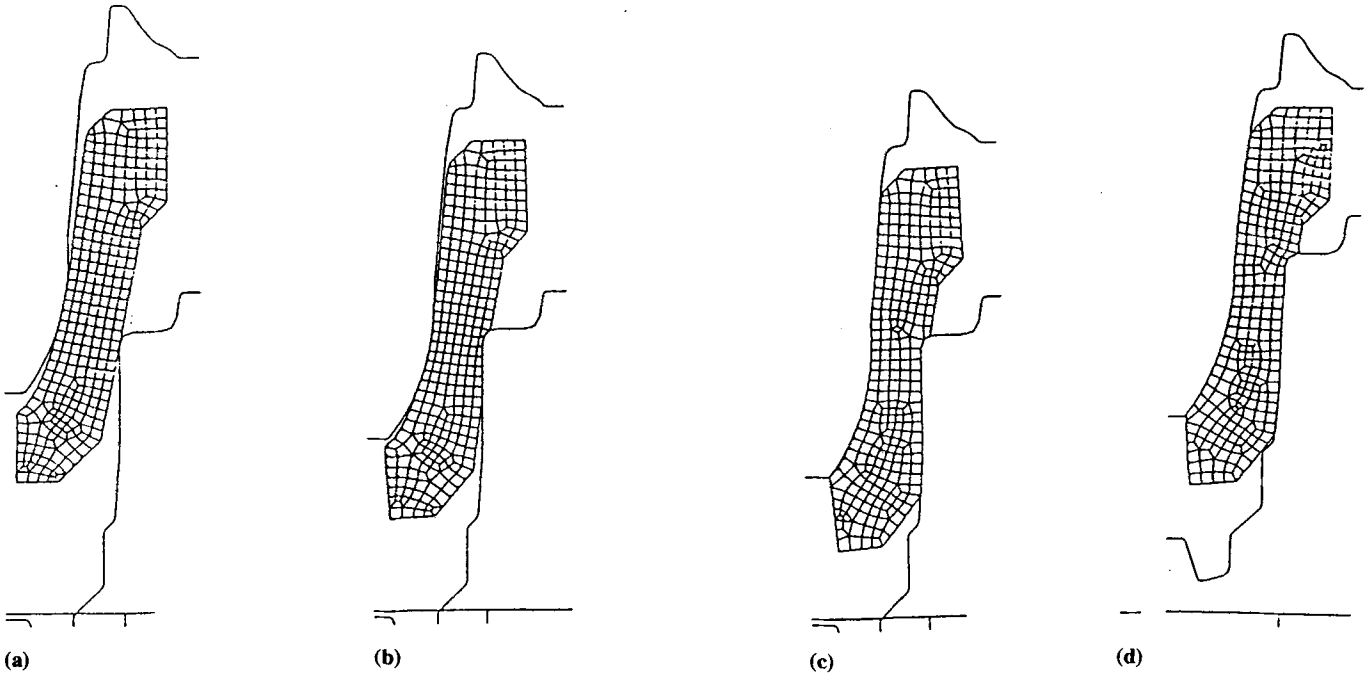

Fig. 9 Forward simulation of the forging of the ball-joint socket showing the shearing of material along the lower die wall

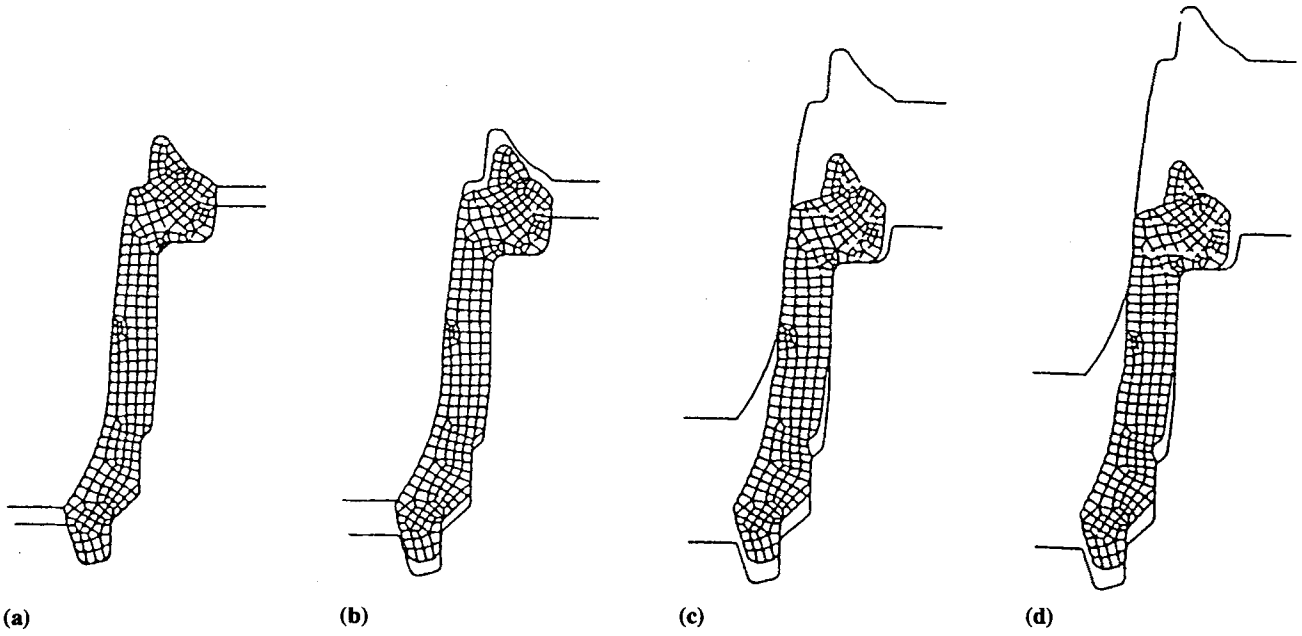

Fig. 10 Finite element grid shapes during backward deformation simulation, using BDOM, from the final forged shape of the ball-joint socket

These differences can be attributed to the use of the force detachment criterion on the bottom die and the influence of the bottom die on the deformation. Figures 7(a) to (c) show the simulation of the deformation up to the intermediate stage using ALPID. Figures 7(d) to (f) show the second stage of forging. The domain was remeshed between the two stages of

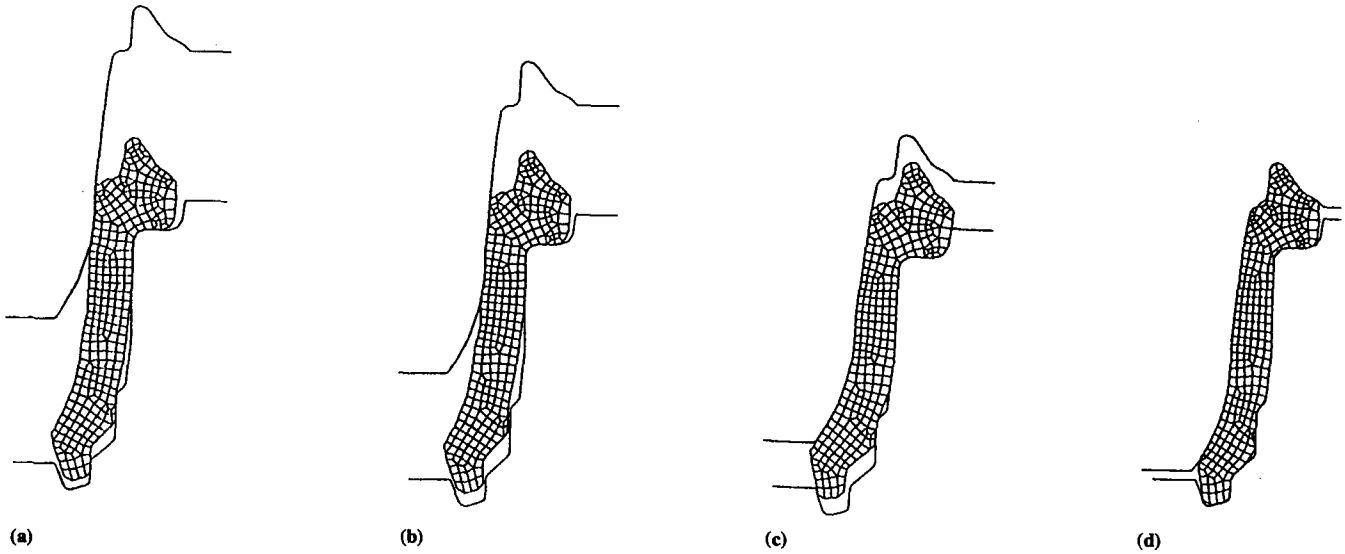

Fig. 11 Forward simulation of the ball-joint socket forging from the optimized intermediate shape

forging. These figures show that complete die fill is obtained without fold over.

3.2 *Forging of an Automotive Ball-Joint Socket*

Figure 8b shows an automotive ball-joint socket, which is typically cold forged from a simpler cup shape shown in Fig. 8a. Simulation of this forging operation, shown in Fig. 9, indicates that, for the particular geometry illustrated, there is shearing of the material along the lower die as the material flows into the annular region between the two dies. The strain rate in the region of the shear was predicted to be considerably higher than elsewhere in the workpiece, and the deformation was quite nonuniform. Such a flow of material could lead to tearing and the formation of surface cracks in the forged part. It also would lead to excessive die wear. These problems were addressed by designing an intermediate shape using BDOM. Figure 10a shows the starting mesh for backward deformation. The 104 nodes in contact with the dies were grouped into 4 segments each along the top and bottom dies. Figure 10 shows the development of this intermediate shape. Strain-rate based nodal detachment was used for the upper die whereas force-based nodal detachment was used for the lower die. Figure 10d shows the optimum intermediate shape.

The shapes of the dies for the intermediate stage were obtained by smoothing the mesh geometry shown in Fig. 10d. The successful design of the intermediate shape is reflected in Fig. 11, which shows the forward simulation from the smoothed intermediate shape to the final shape. The deformation occurs without shearing of the material along the die surface.

4. Summary

A new technique for the design of intermediate shapes in forging is presented in this paper. This method uses optimization techniques and finite element simulation to select a particular path to go back from a final forging shape to an intermediate shape. Optimization techniques were used to extend previously developed backward tracing schemes to arbitrary die shapes. The overall objective of BDOM was to obtain uniform deformation by reducing the variation in accumulated plastic strain. This objective was achieved by minimizing strain-rate variation during deformation. Examples of disk and ball-joint forging considered in this paper show that BDOM is an effective tool for designing intermediate shapes.

Acknowledgment

Support from the Edison Materials Technology Center (EMTEC) through Project CT-19 is acknowledged. This paper was presented at the symposium, "Computer Applications in Shaping and Forming of Materials," held at the annual meeting of TMS in Denver, CO, February 21-25, 1993, and published in the proceedings.

References

1. J.-P. Tang, S.-I. Oh, and T. Altan, The Application of Expert Systems to Automatic Forging Design, *Proceeding of the Thirteenth NAMRC*, NAMRI, Dearbon, MI, 1985, p 456-463
2. W.A. Knight, Part Family Methods for Bulk Metal Forming, *Intl. J. of Production Research*, Vol 12 (No. 2), 1974, p 209-231
3. T.L. Subramaniam, N. Akgerman, and T. Altan, Application of Computer Aided Design and Manufacturing to Precision Isothermal Forging of Titanium Alloys, *Technical Report No. AFML-TR-77-108*, Vol I, II, and III, U.S. Air Force Materials Laboratory, 1977
4. T.L. Subramaniam, N. Akgerman, and T. Altan, Computer Aided Preform Design for Precision Isothermal Forging, *Proceeding of the Fifth NAMRC*, NAMRI, Dearborn, MI, 1977, p 198-213
5. C.H. Lee and S. Kobayashi, New Solution to Rigid Plastic Deformation Problems using a Matrix Method, *J. Eng. Ind. Trans. ASME*, Vol 95, 1973, p 865-873
6. S.-I. Oh, Finite Element Analysis of Metal Forming Processes with Arbitrarily Shaped Dies, *Int. J. Mech. Sci.*, Vol 24 (No. 8), 1982, p 479-493

7. S. Kobayashi, S.-I. Oh, and T. Altan, *Metal Forming and the Finite Element Method*, Oxford University Press, 1989

8. S.M. Hwang and S. Kobayashi, Preform Design in Disk Forging, *Int. J. Machine Tool Design*, Vol 26 (No. 3), 1986, p 231-243

9. S.M. Hwang and S. Kobayashi, Preform Design in Shell Nosing at Elevated Temperatures, *Int. J. Machine Tool Design*, Vol 27 (No. 1), 1987, p 1-14

10. R.V. Grandhi, R. Srinivasan, and C.S. Han, Design of Intermediate Shapes in Forging: Volume II: Development of the Backward Deformation Optimization Method for Forgings, *EMTEC/CT-19/TR-92-19*, Edison Materials Technology Center (EMTEC), 1992

11. C. Han, R.V. Grandhi, and R. Srinivasan, Optimum Design of Forging Die Shapes for Nonlinear Finite Element Analysis, *AIAA Journal*, Vol 31, (No 4), 1993, p774-781